Universality class of the restricted solid-on-solid model with hopping

Su-Chan Park,[1] Jeong-Man Park,[2] and Doochul Kim[1]
[1]*School of Physics, Seoul National University, Seoul 151-747, Korea*
[2]*Department of Physics, Catholic University of Korea, Puchon 420-743, Korea*
(Received 15 August 2001; published 11 February 2002)

We study the restricted solid-on-solid (RSOS) model with finite hopping distance l_0, using both analytical and numerical methods. Analytically, we use the hard-core bosonic field theory developed by the authors [Phys. Rev. E **62**, 7642 (2000)] and derive the Villain-Lai-Das Sarma (VLD) equation for the $l_0=\infty$ case, which corresponds to the conserved RSOS (CRSOS) model and the Kardar-Parisi-Zhang (KPZ) equation for all finite values of l_0. Consequently, we find that the CRSOS model belongs to the VLD universality class and that the RSOS models with any finite hopping distance belong to the KPZ universality class. There is no phase transition at a certain finite hopping distance contrary to the previous result. We confirm the analytic results using the Monte Carlo simulations for several values of the finite hopping distance.

DOI: 10.1103/PhysRevE.65.036108 PACS number(s): 05.90.+m, 81.10.Aj

I. INTRODUCTION

In recent years, the field of nonequilibrium surface growth has been investigated using various discrete models and continuous equations [1]. The comprehension of nonequilibrium surface growth plays an important role in understanding and controlling many interesting interface processes, such as vapor deposition [2], crystal growth [3], molecular beam epitaxy (MBE) [4], and so on. During the MBE growth process, the conserved growth condition is applied without defects, such as overhangs and vacancies. Various discrete conserved models for MBE, describing the kinetic properties of this type of surface growth, have been proposed and studied by intensive numerical simulations.

The main purpose of studying discrete models is to measure scaling exponents for the kinetic roughening, which determines the asymptotic behavior of surface growth on a large length scale in a long time limit. The important result of the kinetic roughening studies is that a large variety of different discrete growth models can be divided into only a few universality classes. The surface width W, which measures the root-mean-square fluctuation of the surface height, scales as

$$W(L,t)\sim L^{\alpha}f(t/L^{z}), \tag{1}$$

where the asymptotic behavior of the scaling function $f(x)$ is constant for $x\gg 1$ and x^{β} for $x\ll 1$ with $\beta=\alpha/z$. The scaling behavior of the growth is characterized by three exponents: the roughness exponent α, the growth exponent β, and the dynamical exponent z. These exponents determine the universality class.

In the coarse-grained picture, evolution of the growing surface is usually described by a stochastic differential equation (SDE) for the height variable $h(\mathbf{x},t)$ as a function of the surface coordinate and time. For discrete models of MBE growth, several SDEs were suggested and it was generally believed that there is a correspondence between discrete growth models and continuum SDEs. The common way of establishing the link between discrete models and continuous equations is a simple comparison of critical exponents determined from computer simulations of the discrete model with exponents for the continuous equation.

There have also been attempts to establish the correspondence in an explicit way. The systematic procedure for establishing a continuous equation corresponding to discrete models, starting from the master equation in discrete space was proposed by Vvedensky *et al.* [5] and has been successfully applied to the derivation of growth equations for some discrete models, including the solid-on-solid (SOS) model, the restricted solid-on-solid (RSOS) model, as well as the Wolf-Villain and Das Sarma-Tamborenea models [6–8]. However, there are several difficulties with this procedure; in particular, in converting from the equation system for a discrete set of heights to an equation for a continuous function $h(\mathbf{x},t)$, the procedure requires the regularization step, in which the nonanalytic quantities are expanded and replaced with analytic quantities, i.e., the step function is approximated by an analytic shifted hyperbolic tangent function expanded in a Taylor series. However, the form of the regularized function is uncertain, and different choices of this function lead to different results. Some forms of the regularized function have been suggested, but the problem of a proper choice of a regularization scheme has not been discussed.

To overcome this kind of uncertainty, the authors proposed a new schematic formalism [9], deriving the continuous equations, such as the Edwards-Wilkinson (EW) [10] and Kardar-Parisi-Zhang (KPZ) [11] equations, from the body centered solid-on-solid model and the RSOS model. In this paper, we apply our formalism to a new kind of MBE growth model proposed by Kim, Park, and Kim [12]. This model allows the deposited particle to relax to the nearest site where the RSOS condition on neighboring heights is satisfied and has the conserved growth condition constraint, which means the deposited particles are possible to hop for an infinite distance until they eventually find the site with the RSOS condition satisfied. Applying our formalism to the above conserved RSOS (CRSOS) model, we not only derive the Villain-Lai-Das Sarma (VLD) equation [13] for the

model which belongs to a different universality class from the EW and KPZ equations, but also we are able to predict the coefficients in the VLD equation, which was not possible by other methods.

Observing that the RSOS model belongs to the KPZ class and the CRSOS model belongs to the VLD class, we went one step further to study the RSOS model with the finite range hopping (RSOS/H). In this RSOS/H model, it is possible for the deposited particles to hop a finite distance l_0 until they find the site with the RSOS condition satisfied. If they fail to find the site with the RSOS condition satisfied within the distance l_0 in both directions, the deposition process is rejected. The RSOS model corresponds to the RSOS/H model with $l_0=0$ and to the CRSOS model with $l_0=\infty$. We apply our formalism to the RSOS/H model with l_0 finite and find that this model belongs to the KPZ class, contrary to the previous report by Kim and Yook [14], who concluded that there is a phase transition between the KPZ class to the VLD class along the parameter l_0.

In Sec. II our formalism to derive the continuous equation from the discrete model is briefly explained and the procedure of derivation is described. The detailed calculations are attached in the appendices. Extensive numerical simulations are presented in Sec. III and the summary and discussion are given in Sec. IV.

II. DERIVATION OF THE STOCHASTIC EQUATION

In this section, we derive continuous equations for the one-dimensional RSOS/H model with a hopping distance l_0 and for the CRSOS model corresponding to $l_0=\infty$. We restrict ourselves to the case wherein the height difference between two nearest neighbors is not larger than 1. For a succinct description of the dynamics, we introduce the nomenclature that if a site m satisfies the condition $|h_m+1-h_{m\pm1}|\leqslant 1$, this site is called "stable." Following this nomenclature, the growth algorithm of the one-dimensional RSOS/H model is as follows: (i) We choose a site m randomly. (ii) Sites from $m-l_0$ to $m+l_0$ are examined to determine if they are stable sites. (iii) If a stable site is found within the interval from $m-l_0$ to $m+l_0$, a new particle is deposited to the nearest stable site from m (m itself can be a candidate for deposition). However, if stable sites are nonexistent in the examined interval, the particle drop is rejected and the system remains unchanged. After this try, the time is increased by $1/L$, where L is the system size. We assume periodic boundary conditions.

Since the height difference between two nearest neighbors is restricted not to be larger than 1, the RSOS/H model is mapped onto the reaction-diffusion system of hard-core particles with two species. The step-up (-down) is mapped to an $A(B)$ particle. If two nearest neighbor sites have equal height, a particle vacuum is located between these two sites. The site where the particles reside is labeled by an integer, and the site for height by a half-integer. This mapping is depicted in Fig. 1. According to this mapping, the dynamics of the RSOS/H model can be described by the (imaginary time) Schrödinger equation $(\partial/\partial t)|\Psi;t\rangle=-\hat{H}|\Psi;t\rangle$ for the state vector $|\Psi;t\rangle\equiv\Sigma_C P(C;t)|C\rangle$, where $P(C;t)$ is the probability with which the system is in state C at time t, and $\hat{H}$, called a Hamiltonian, is an evolution operator

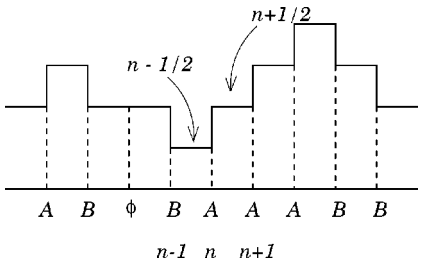

FIG. 1. Relation of species to the height slope. We use the integer to indicate the location of particles and the half-integer for the height configuration. Hence the RSOS condition at site $n+\frac{1}{2}$ is determined by the situation at sites n and $n+1$.

$$\hat{H}=\sum_n (\hat{I}-\hat{R}_n-\hat{A}_n)\hat{L}_n, \tag{2}$$

where

$$\hat{L}_n=\hat{I}+\frac{1}{2}\sum_{j=1}^{2l_0}\left(\prod_{k=1}^{j}\hat{R}_{n+k}+\prod_{k=1}^{j}\hat{R}_{n-k}\right), \tag{3}$$

and

$$\hat{R}_n=\hat{a}_n^\dagger\hat{a}_n+\hat{b}_{n+1}^\dagger\hat{b}_{n+1}-\hat{a}_n^\dagger\hat{a}_n\hat{b}_{n+1}^\dagger\hat{b}_{n+1},$$

$$\hat{A}_n=(\hat{a}_n^\dagger+\hat{b}_n)(\hat{a}_{n+1}+\hat{b}_{n+1}^\dagger). \tag{4}$$

The role of the rejection operator $\hat{R}_n$ is to check the stability of site $n+\frac{1}{2}$, that is, if a configuration $|C\rangle$ has a stable site at $n+\frac{1}{2}$, $\hat{R}_n|C\rangle=0$ and otherwise $\hat{R}_n|C\rangle=|C\rangle$. The adsorption operator $\hat{A}_n$ describes the configuration change after a successful deposition. $\hat{a}_n(\hat{b}_n)$ is the annihilation operator of an $A(B)$ particle at site n and $\hat{a}_n^\dagger(\hat{b}_n^\dagger)$ is the corresponding creation operator, satisfying the mixed commutation relations presented in Ref. [9],

$$\hat{a}_n\hat{a}_n^\dagger=\hat{b}_n\hat{b}_n^\dagger=\hat{I}-\hat{a}_n^\dagger\hat{a}_n-\hat{b}_n^\dagger\hat{b}_n, \quad \hat{a}_n\hat{b}_n=\hat{a}_n^\dagger\hat{b}_n^\dagger=0. \tag{5}$$

All operators at different sites commute with each other.

To find the SDE for the RSOS/H model, we apply the method recently introduced by the authors [9]. First we assume the existence of the lattice version of the SDEs in terms of density. Those equations are supposed to take the forms

$$\partial_t a_n=C_n^A(\{a\},\{b\})+\sum_m [g_{nm}^{AA}\xi_m^A(t)+g_{nm}^{AB}\xi_m^B(t)], \tag{6}$$

$$\partial_t b_n=C_n^B(\{a\},\{b\})+\sum_m [g_{nm}^{BA}\xi_m^A(t)+g_{nm}^{BB}\xi_m^B(t)], \tag{7}$$

where $\partial_t\equiv\partial/\partial t$ and ξ_n^A, ξ_n^B are white noises with correlation

$$\langle \xi_n^X(t)\xi_m^{X'}(t')\rangle = \delta_{nm}\delta_{X,X'}\delta(t-t')$$

$$(X,X' = \text{either } A \text{ or } B), \tag{8}$$

where δ_{nm} and $\delta_{X,X'}$ are Kronecker deltas and $\delta(t-t')$ is the Dirac delta function. The matrix g is related to the Kramers-Moyal coefficient in such a way that

$$\sum_{r,X''} g_{nr}^{XX''} g_{mr}^{X'X''} = C_{nm}^{XX'}(\{a\},\{b\})$$

$$(X,X',X'' = \text{either } A \text{ or } B). \tag{9}$$

Here we are using the Itô interpretation. The field $a(b)$ in the curly bracket represents the density of species $A(B)$ at all sites. From here on, without a hat above itself a mathematical symbol is a pure number as opposed to an operator. a_n should not be confused with $\hat{a}_n$. The former is a density at site n that runs over real numbers, while the latter is an annihilation operator. By requiring that the noise average of observables in Eqs. (6) and (7) has the same behavior with the ensemble average of the number operator, we find [9]

$$\langle C_n^A\rangle_t = \langle [H,\hat{a}_n^\dagger \hat{a}_n]\rangle_t,$$

$$\langle C_n^B\rangle_t = \langle [H,\hat{b}_n^\dagger \hat{b}_n]\rangle_t,$$

$$\langle C_{nm}^{AA}\rangle_t = \langle [\hat{a}_n^\dagger \hat{a}_n,[H_i \hat{a}_m^\dagger \hat{a}_m]]\rangle_t, \tag{10}$$

$$\langle C_{nm}^{AB}\rangle_t = \langle C_{mn}^{BA}\rangle_t = \langle [\hat{a}_n^\dagger \hat{a}_n,[H,\hat{b}_m^\dagger \hat{b}_m]]\rangle_t,$$

$$\langle C_{nm}^{BB}\rangle_t = \langle [\hat{b}_n^\dagger \hat{b}_n,[H,\hat{b}_m^\dagger \hat{b}_m]]\rangle_t,$$

where the $\langle\cdots\rangle_t$ on the left hand side represents the average over noise at time t and that on the right hand side stands for the ensemble average. The arguments of the Kramers-Moyal coefficients are dropped for brevity.

As presented in Ref. [9], the ensemble average of any operator can be interpreted as an average of number operators due to the property of the projection state $\langle\cdot|$, which is defined as a sum over all possible microscopic configurations and is itself a left eigenstate of $\hat{H}$ with eigenvalue 0, and in turn, the ensemble average of a number operator is mapped to the noise average of density. This procedure leads us to find the Kramers-Moyal coefficients C_n^X, C_{nm}^{XY}, in terms of the density fields. We call this procedure *figurization*, which means ''expression in number.'' To represent the *figurization*, we use the symbol $\mapsto$ to the left of which is an operator (or a product of operators) and to the right of which is the corresponding density representation.

To complete the derivation, we perform the commutation relations between the Hamiltonian and the density operators and so forth;

$$[\hat{H},\hat{a}_n^\dagger \hat{a}_n] = \hat{a}_n^\dagger(\hat{a}_{n+1}+\hat{b}_{n+1}^\dagger)\hat{L}_n - \hat{a}_n(\hat{a}_{n-1}^\dagger+\hat{b}_{n-1})\hat{L}_{n-1}, \tag{11}$$

$$[\hat{H},\hat{b}_n^\dagger \hat{b}_n] = -\hat{b}_n(\hat{a}_{n+1}+\hat{b}_{n+1}^\dagger)\hat{L}_n + \hat{b}_n^\dagger(\hat{a}_{n-1}^\dagger+\hat{b}_{n-1})\hat{L}_{n-1}, \tag{12}$$

$$[\hat{a}_l^\dagger \hat{a}_l,[\hat{H},\hat{a}_n^\dagger \hat{a}_n]]$$
$$= \delta_{ln}(\hat{a}_n^\dagger(\hat{a}_{n+1}+\hat{b}_{n+1}^\dagger)\hat{L}_n + \hat{a}_n(\hat{a}_{n-1}^\dagger+\hat{b}_{n-1})\hat{L}_{n-1})$$
$$- \delta_{l,n+1}\hat{a}_n^\dagger \hat{a}_{n+1}\hat{L}_n - \delta_{l,n-1}\hat{a}_n \hat{a}_{n-1}^\dagger \hat{L}_{n-1}, \tag{13}$$

$$[\hat{b}_l^\dagger \hat{b}_l,[\hat{H},\hat{b}_n^\dagger \hat{b}_n]]$$
$$= \delta_{ln}(\hat{b}_n(\hat{a}_{n+1}+\hat{b}_{n+1}^\dagger)\hat{L}_n + \hat{b}_n^\dagger(\hat{a}_{n-1}^\dagger+\hat{b}_{n-1})\hat{L}_{n-1})$$
$$- \delta_{l,n+1}\hat{b}_n \hat{b}_{n+1}^\dagger \hat{L}_n - \delta_{l,n-1}\hat{b}_n^\dagger \hat{b}_{n-1}\hat{L}_{n-1}, \tag{14}$$

$$[\hat{a}_l^\dagger \hat{a}_l,[\hat{H},\hat{b}_n^\dagger \hat{b}_n]] = \delta_{l,n+1}\hat{b}_n \hat{a}_{n+1}\hat{L}_n + \delta_{l,n-1}\hat{b}_n^\dagger \hat{a}_{n-1}^\dagger \hat{L}_{n-1}, \tag{15}$$

where δ_{nl} is a Kronecker delta. Following the *figurization*, we find the Kramers-Moyal coefficients. For a later purpose, we give some examples of the figurization. The figurization of $\hat{R}_n$ is $\hat{R}_n \mapsto R_n \equiv a_n + b_{n+1} - a_n b_{n+1}$, and the symbolic representation of the figurization of the product of $\hat{R}$'s is

$$\prod_{k=1}^{j} \hat{R}_{n+k} \mapsto R_n^j, \tag{16}$$

where the superscript j should not be confused with the power. When $j=1$, R_n^1 is denoted as R_{n+1}. R_n^j are given by the following recursion relations:

$$R_n^j = a_{n+1}R_{n+1}^{j-1} + (1-a_{n+1})\prod_{k=2}^{j+1} b_{n+k}, \tag{17}$$

$$R_{n-j-2}^j = b_{n-1}R_{n-j-2}^{j-1} + (1-b_{n-1})\prod_{k=2}^{j+1} a_{n-k}, \tag{18}$$

where $j \geqslant 1$ and we define $R_n^0 \equiv 1$. The physical meaning of Eqs. (17) and (18) is as follows: We divide the situation that prohibits the height increase at sites $n+\frac{3}{2}, n+\frac{5}{2}, \ldots, n+j+\frac{1}{2}$ by the condition at site $n+1$. If there is an A particle at site $n+1$, the height increase is suppressed at site $n+\frac{3}{2}$ irrespective of the condition at site $n+2$. Hence the first term of Eq. (17) follows. If there is no A particle at site $n+1$, to suppress the deposition at site $n+\frac{3}{2}$, there must exist a B particle at site $n+2$ and this should be continued until the site $n+j+1$, because at site $n+k(2 \leqslant k \leqslant j)$ no A particle is present; this condition is represented by the second term. To comprehend Eq. (18), we only have to perform the mirror transformation relative to site n. By the mirror transformation relative to a site n, we mean the exchange of a and b $(a \leftrightarrow b)$, followed by $n+k \leftrightarrow n-k$. Under this transformation, R_{n+k}^j changes into $R_{n-k-j-2}^j$ for an arbitrary k. The mirror transformation of Eq. (17) is Eq. (18).

With these notions, we will find the SDE of the RSOS/H model. At first, the deterministic part of SDE is found. Since the main concern is not the respective dynamics of the A and B particles, but it is $D_n \equiv a_n - b_n$ (the local slope) and $S_n = a_n + b_n$ (the slope density), we will write the SDE for D and S rather than for the A, B particles. The Kramers-Moyal

coefficient C_n^D is obtained by subtracting Eq. (12) from Eq. (11) and C_n^S by adding Eq. (12) and (11) followed by the *figurization*.

$$C_n^D=\tfrac{1}{2}\sum_{j=1}^{2l_0}[R_{n-2}^j-2R_{n-1}^j+R_n^j-(R_{n-j-2}^j-2R_{n-j-1}^j+R_{n-j}^j)]+\tfrac{1}{2}(R_{n-2}^{2l_0+1}-R_{n-l}^{2l_0+1}+R_{n-2l_0-2}^{2l_0+1}-R_{n-2l_0-1}^{2l_0+1}), \tag{19}$$

$$\begin{aligned}C_n^S=&2-3(a_n+b_n)-(b_na_{n+1}+a_nb_{n-1}-3b_nb_{n+1}-3a_na_{n-1})+\tfrac{1}{2}\sum_{j=1}^{2l_0}(R_n^j-R_{n-2}^j-R_{n-j}^j+R_{n-j-2}^j)\\&-b_n(1-S_{n+1})b_{n+2}-a_n(1-S_{n-1})a_{n-2}\\&-\tfrac{1}{2}(R_{n-1}^{2l_0+1}+R_{n-2l_0-1}^{2l_0+1}+R_{n-2}^{2l_0+1}+R_{n-2l_0-2}^{2l_0+1})\\&-\sum_{j=1}^{2l_0-1}\left[b_na_{n+1}R_{n+1}^j+b_n(1-S_{n+1})\prod_{k=2}^{j+2}b_{n+k}+b_n(1-b_{n+1})R_{n-j-2}^j\right]-\sum_{j=1}^{2l_0-1}\left[a_nb_{n-1}R_{n-j-3}^j+a_n(1-S_{n-1})\prod_{k=2}^{j+2}a_{n-k}+a_n(1-a_{n-1})R_n^j\right].\end{aligned} \tag{20}$$

As pointed out in Ref. [15], the mass term in Eq. (20) makes the step density saturate fast. As a result, the step density S becomes a slave field of the slope D takes the form

$$S=2\rho(l_0)+\mu_0(l_0)\partial D+\theta_0(l_0)D^2+\cdots, \tag{21}$$

where $2\rho(l_0)$ is the (mean-field) stationary step density and μ_0 and θ_0 may depend on l_0. Here $\partial\equiv\partial/\partial_x$. Since this system has the mirror symmetry whose continuum version is invariant under the transformations $D\to -D$ and $\partial\to-\partial$, we do not expect the occurrence of D in Eq. (21). The parameters $\rho(l_0)$, $\mu_0(l_0)$, and $\theta_0(l_0)$ are determined by the stationarity of Eq. (20). In Appendix A, we obtain ρ, θ_0, and μ_0 as functions of l_0 and show the approximate solutions of these parameters. We can now rewrite Eq. (19) in terms of the height field h using Eq. (21) and

$$D=\partial h. \tag{22}$$

The last task is to determine the noise strength. This is accomplished using Eqs. (6) and (7). After eliminating S in favor of D, there is only one kind of noise with strength

$$C_{nm}=C_{nm}^{AA}+C_{nm}^{BB}-C_{nm}^{AB}-C_{nm}^{BA}. \tag{23}$$

Using *figurization* of Eq. (10) and keeping the most relevant term, we find

$$C_{nm}=-(1-\rho)^2L(\delta_{n,m+1}-2\delta_{nm}+\delta_{n,m-1})+\cdots, \tag{24}$$

where

$$L=\sum_{l=0}^{2l_0}\rho^l(1+l-\rho l). \tag{25}$$

For finite l_0 we found

$$\partial_t h=v_\infty+\nu\partial^2 h+\frac{\lambda}{2}(\partial h)^2+\xi(x,t), \tag{26}$$

$$\langle\xi(x,t)\xi(x',t')\rangle=D_{\xi\xi}\delta(x-x')\delta(t-t'),$$

where

$$\begin{aligned}v_\infty&=1-R(2l_0+1)\simeq 1-\rho_\infty^{2l_0}[\tfrac{1}{2}+(\sqrt{2}-1)l_0]+O(\rho_\infty^{4l_0}),\\ \nu&=-\mu(2l_0+1)\\&\simeq\rho_\infty^{2l_0}(l_0+1)(2l_0+1)\left(\frac{\sqrt{2}}{6}l_0+\frac{3-\sqrt{2}}{4}\right)+O(\rho_\infty^{4l_0}),\\ \lambda&=-2\theta(2l_0+1)\\&\simeq-\rho_\infty^{2l_0}(1+l_0)(1+2l_0)\left(1+\frac{\sqrt{2}+1}{3}l_0\right)+O(\rho_\infty^{4l_0}),\\ D_{\xi\xi}&\simeq\frac{2\sqrt{2}-1}{2}\left[1-\rho_\infty^{2l_0}\left(\frac{6+5\sqrt{2}}{28}+\frac{19\sqrt{2}-22}{14}l_0\right)\right]+O(\rho_\infty^{4l_0}),\end{aligned} \tag{27}$$

with $\rho_\infty=(2-\sqrt{2})/2$. The numerical values of $\rho(l_0)$, $\nu(l_0)$, and $\lambda(l_0)$ are given for several values of l_0 in Table I. For infinite l_0

$$\partial_t h=\tilde{v}_\infty-\tilde{\nu}\partial^4 h+\tilde{\lambda}\partial^2(\partial h)^2+\tilde{\xi}(x,t), \tag{28}$$

$$\langle\tilde{\xi}(x,t)\tilde{\xi}(x',t')\rangle=\tilde{D}_{\xi\xi}\delta(x-x')\delta(t-t'),$$

where

$$\tilde{v}_\infty=1,\qquad\tilde{\nu}=\frac{21-12\sqrt{2}}{2},\qquad\tilde{\lambda}=\frac{10-3\sqrt{2}}{2},\qquad\tilde{D}_{\xi\xi}=\frac{2\sqrt{2}-1}{2}. \tag{29}$$

Equation (26) directly shows that the RSOS/H model, for any finite l_0, belongs to the KPZ class, and Eq. (28) suggests that the CRSOS model is described by the VLD equation. However, the first line of Eq. (19) has the form

TABLE I. Numerical values of $\rho(l_0)$, $\nu(l_0)$, and $\lambda(l_0)$.

l_0	$\rho(l_0)$	$\nu(l_0)$	$\lambda(l_0)$
0	$\frac{1}{3}$	$\frac{1}{3}$	$\frac{-5}{6}$
1	0.299 027 750 50	3.3887×10^{-1}	-9.5709×10^{-1}
2	0.293 696 759 81	9.7310×10^{-2}	-2.9204×10^{-1}
3	0.292 988 255 45	1.9569×10^{-2}	-6.0527×10^{-2}
4	0.292 903 676 47	3.2656×10^{-3}	-1.0287×10^{-2}
5	0.292 894 314 95	4.8299×10^{-4}	-1.5406×10^{-3}
6	0.292 893 329 94	6.5674×10^{-5}	-2.1140×10^{-4}
7	0.292 893 229 81	8.3964×10^{-6}	-2.7217×10^{-5}
8	0.292 893 219 88	1.0242×10^{-6}	-3.3380×10^{-6}
9	0.292 893 218 92	1.2038×10^{-7}	-3.9408×10^{-7}
10	0.292 893 218 82	1.3730×10^{-8}	-4.5115×10^{-8}
⋮	⋮	⋮	⋮
∞	0.292 893 218 81	0	0

$$\sum_{j=1}^{2l_0}\left[R^j_{n-2}-2R^j_{n-1}+R^j_n - \{\text{mirror terms of } (R^j_{n-2}-2R^j_{n-1}+R^j_n)\}\right], \tag{30}$$

which has the following implications: If the continuum version of $R^j_{n-2}-2R^j_{n-1}+R^j_n$ has a nonvanishing coefficient of $\partial^2(D^{2r+1})$ with a non-negative integer r, it is not certain that Eq. (30) is a lattice version of ∂^3; consider the mirror transformation in the continuum limit. The occurrence of $\partial^2(D^{2r+1})$ in Eq. (30) is directly related to the appearance of $\partial(\partial h)^{2r+1}$ in Eq. (28), which generates an EW term by the dynamic renormalization group [16]. Appendix B shows that this is not the case. The vanishing of D^{2r+1} in the continuum limit of R^j_{n+k} guarantees the vanishing of $\partial^2(D^{2r+1})$ in $R^j_{n-2}-2R^j_{n-1}+R^j_n$. In view of this, we conclude that the continuum equation of the CRSOS model is the VLD equation.

To confirm this conclusion, we have performed Monte Carlo simulations as outlined in Sec. III.

III. NUMERICAL STUDY

Although the RSOS/H model was studied numerically by Kim and Yook [14], their results are contradictory to our derivation. As a result, we need to perform extensive numerical simulations to verify our results. In the derivation, we found that the coefficients of the EW terms and the KPZ terms are vanishingly small, though finite, for large l_0. Hence, we may find a crossover of roughness exponents from VLD ($\alpha_{\rm vld}\simeq0.95$) to KPZ ($\alpha_{\rm kpz}=0.5$). We are preoccupied with the numerical observation of this crossover.

In Fig. 2, we draw the saturated width $W_{\rm sat}$ as function of the system size L for some l_0's. The system sizes are 64, 90, 128, 180, 256, 360, 512, 720, and 1024. For relatively small system sizes, the roughness exponents are near to the values reported in Ref. [14]. As expected from our derivation, we see a crossover for large system sizes.

To clarify the crossover behavior, a scaling plot is given in Fig. 3. The anticipated scaling form of the saturated width is

$$W_{\rm sat}(l_0,L)=L^{\alpha_{\rm vld}}g(l_0^{\gamma}/L), \tag{31}$$

where γ is the crossover exponent. The asymptotic behavior of the scaling function g is expected to be

$$g(x)\sim\begin{cases}\text{const} & \text{when } x\to\infty,\\ x^{\alpha_{\rm vld}-\alpha_{\rm kpz}} & \text{when } x\to0.\end{cases} \tag{32}$$

The best fit for the data set shown in Fig. 2 corresponds to $\alpha_{\rm vld}=0.9$ and $\gamma=2.0$. The fitting parameter $\alpha_{\rm vld}$ obtained is somewhat smaller than the known value of the roughness

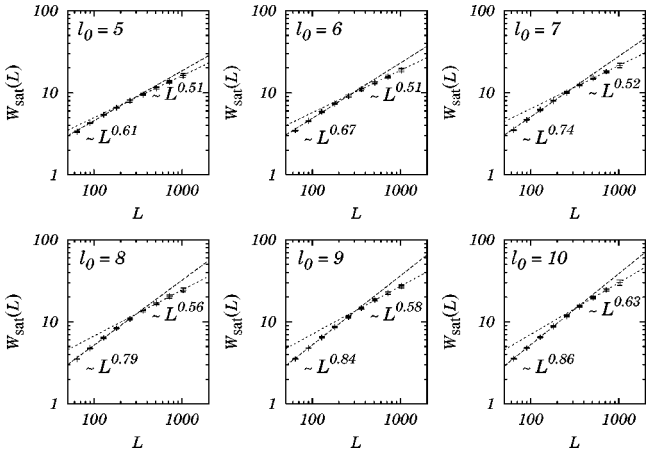

FIG. 2. Plots for the saturation width as a function of the system size for various l_0. We find the saturation width by a least-squares fit and the error bars represent three times the standard deviation, which includes 99% of the data. We fit the data as a function of L and find two exponents. The exponents for the smaller system sizes are written in the bottom left and those of the larger system sizes in the upper right. The lines show the fitting results. Up to 512, it seems plausible to insist that the systems are in the scaling regime, but the data for 1024 show the clear discrepancy within an error bar.

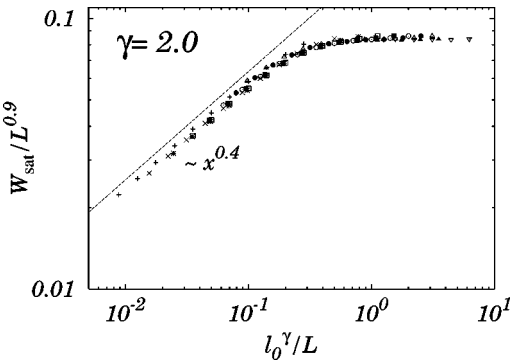

FIG. 3. Scaling plot of saturated widths of the one-dimensional RSOS/H model. The scaling variable is l_0^{γ}/L. The values of l_0 are equal to those in Fig. 2. We also draw the line $x^{\alpha_{\rm vld}-\alpha_{\rm kpz}}=x^{0.4}$ as a guide to the eye.

exponent of the CRSOS model. This is most likely due to the smallness of l_0. For example, the data for $l_0=10$ in Fig. 2 yield 0.86 rather than 0.95. The meaning of γ is as follows: When the system size is sufficiently large, we expect the width of the characteristic mountain to be $\sim L^{\alpha_{\rm kpz}}$. Due to the RSOS condition, the linear size of the mountain is also expected to be $\sim L^{\alpha_{\rm kpz}}$. The smaller the system size, the less the rejection events occur due to the shrinking of the characteristic mountain. If l_0 is comparable with the linear size of the characteristic mountain ($L^{\alpha_{\rm kpz}}$), the system starts to behave differently. Eventually, the system with small size, $L^{\alpha_{\rm kpz}} \ll l_0$, cannot feel the existence of l_0. Thus the crossover length L^* is expected to be $l_0^{1/\alpha_{\rm kpz}}$, that is, $\gamma=1/\alpha_{\rm kpz}=2$.

IV. SUMMARY AND DISCUSSION

We studied the RSOS/H model using both analytical and numerical methods. We derived the continuum equation for the microscopic discrete model analytically, and found coefficients of the EW term $\partial^2 h$, the KPZ term $(\partial h)^2$, as well as the VLD term $\partial^2(\partial h)^2$. We observed that the coefficients of the EW and KPZ terms behave as $\sim a_0^{2l_0} l_0^3$ for sufficiently large l_0, which is consistent with the previous numerical study [14]. Accordingly, we concluded that the RSOS/H model for any finite l_0 eventually belongs to the KPZ class and the CRSOS model belongs to the VLD class. Numerically, we reported the crossover from the VLD class to the KPZ one, which confirms our derivation. Moreover, we found a crossover exponent γ, which is argued to be 2.

Besides these studies, we can offer an (nonrigorous plausible) argument to anticipate the universality class of the RSOS/H model by employing the block spin concept of Kadanoff's. Consider a system with linear size L and hopping distance l_0. Similar to the block spin in the Ising model, we introduce a coarse-graining parameter b, which blocks the b sites by one. Although the exact transformation of coarse-graining cannot be determined, we expect that if it exists, l_0 may be renormalized as $\sim l_0/b^{\gamma'}$. Hence, we expect that the stable fixed point corresponds to $l_0=0$, which is the KK model [17] and the unstable fixed point corresponds to $l_0=\infty$, which is the CRSOS model [18].

ACKNOWLEDGMENTS

We are grateful to Byungnam Kahng for helpful discussions. This work was supported by Grant No. 2000-2-11200-002-3 from the BRP program of the KOSEF.

APPENDIX A: CONTINUUM LIMIT AND DETERMINATION OF θ_0 AND μ_0

In this appendix, we derive the continuum limit of R^l_{n+k} where n is the reference point. One may obtain the continuum limit directly from Eq. (17), but we do not follow this route. Rather, we make recursion relation about the parameters that appear in front of the field (see below). The use of Eq. (21) makes it possible to represent the continuum limit in terms of D, which is directly related to the height by Eq. (22). We can find the correct coefficient that appears in Eq. (21) after we find the continuum limit of R^l_{n+k}.

The continuum limit of R^l_{n+k} takes the form

$$R^l_{n+k} \doteq R(l)+\gamma(l,k)D+\theta(l,k)D^2+\mu(l,k)\partial D+\cdots, \tag{A1}$$

where the implicit dependence on l_0 is assumed and the argument of D is dropped for simplicity. The symbol "$\doteq$" represents the continuum limit of a quantity. Equation (17) allows us to find the recursion relations. Before going further, the explicit form of $R(l)$ in the case of no tilt boundary condition is found. The recursion relation becomes

$$\begin{aligned} R(l)&=\rho R(l-1)+(1-\rho)\rho^l, \\ \Rightarrow \rho^{-1}R(l)&=\rho^{-(l-1)}R(l-1)+1-\rho \end{aligned} \tag{A2}$$

with an (sort of) initial condition $R(1)=2\rho-\rho^2$. ρ is the abbreviation of $\rho(l_0)$ in Eq. (21). It is trivial to find the solution that reads

$$R(l)=\rho^l+\rho^l(1-\rho)l. \tag{A3}$$

To find the recursion relations, we need a continuum limit of P^k_l, which is defined as

$$P^k_l \equiv (1-a_{n+k+1})\prod_{m=2}^{l+1} b_{n+k+m} = P^k_{l-1} b_{n+k+l+1}. \tag{A4}$$

One may directly calculate the continuum limit of P^k_l, but we follow another path. Let the continuum limit of P^k_l be

$$P^k_l \doteq (1-\rho)\rho^l+\gamma_1(l,k)D+\theta_1(l,k)D^2+\mu_1(l,k)\partial D+\cdots. \tag{A5}$$

From Eq. (A4), we find the recursion relations ($l \geqslant 2$)

$$\begin{aligned} \frac{\gamma_1(l,k)}{\rho^l}&=\frac{\gamma_1(l-1,k)}{\rho^{l-1}}-\frac{1-\rho}{2\rho}, \\ \frac{\theta_1(l,k)}{\rho^l}&=\frac{\theta_1(l-1,k)}{\rho^{l-1}}-\frac{\gamma_1(l-1,k)}{2\pi^l}+\theta_0\frac{1-\rho}{2\rho}, \\ \frac{\mu_1(l,k)}{\rho^l}&=\frac{\mu_1(l-1,k)}{\rho^{l-1}}+(\mu_0-k-l-1)\frac{1-\rho}{2\rho}, \end{aligned} \tag{A6}$$

with initial conditions

$$\gamma_1(1,k)=-\tfrac{1}{2},$$
$$\theta_1(1,k)=\tfrac{1}{4}(1+2\theta_0-4\rho\theta_0), \tag{A7}$$
$$\mu_1(1,k)=\tfrac{1}{2}(\mu_0-\kappa-2-2\rho\mu_0+\rho).$$

θ_0 and μ_0 are functions of l_0 as shown in Eq. (21), which are to be determined by Eq. (20). The solutions of Eq. (A6) under the condition (A7) are ($l\geqslant 1$)

$$\gamma_1(l,k)=\rho^{l-1}\left[\gamma_1(1,k)-\frac{1-\rho}{2}(l-1)\right],$$
$$\theta_1(l,k)=\rho^{l-1}\left[\theta_1(1,k)+\left(\theta_0-\rho\theta_0+\frac{1}{2\rho}\right)\frac{l-1}{2}+\frac{1-\rho}{8\rho}(l-1)(l-2)\right], \tag{A8}$$
$$\mu_1(l,k)=\rho^{l-1}\left[\mu_1(1,k)+\frac{1-\rho}{2}(\mu_0-k-2)(l-1)-\frac{1-\rho}{4}l(l-1)\right].$$

Now we can obtain the continuum limit of R^l_{n+k}. Using Eqs. (17), (A5), and (A8), we find the recursion relations of parameters given in Eq. (A1)

$$\gamma(l,k)=\rho\,\gamma(l-1,k+1),$$
$$\theta(l,k)=\rho\,\theta(l-1,k+1)+\theta_1(l,k)+\frac{\theta_0}{2}\rho^{l-i}[l-\rho(l-1)],$$
$$\mu(l,k)=\rho\mu(l-1,k+1)+\mu_1(l,k)+\frac{\rho^{l-1}}{2}(1+k+\mu_0)[l-\rho(l-1)],$$

with conditions

$$\gamma(1,k)=0,$$
$$\theta(1,k)=\tfrac{1}{4}+\theta_0(1-\rho), \tag{A9}$$
$$\mu(1,k)=(1-\rho)(\mu_0-\tfrac{1}{2}).$$

We solve Eq. (A9) step by step. It is trivial to find that $\gamma(l,k)=0$. As shown in Appendix B, the vanishing of γ is not a coincidence. Since $\theta_1(l,k)$ has no k dependence, we expect that $\theta(l,k)$ also has no k dependence. We find

$$\theta(l)=l\rho^{l-1}\left[\frac{1}{4}+\theta_0(1-\rho)+\left(2\theta_0-2\rho_0+\frac{1}{2\rho}\right)\frac{l-1}{4}+\frac{1-\rho}{24\rho}(l-1)(l-2)\right], \tag{A10}$$

where k is removed from the argument of θ due to the independence. $\mu(l,k)$ seems to have an explicit k dependence, but by inserting $\mu_1(l,k)$ directly, we find the independence of $\mu(l,k)$ on k. The result reads (we drop k by the same reason as θ)

$$\mu(l)=(1-\rho)\rho^{l-1}\frac{l(l+1)}{4}\left(2\mu_0-\frac{l}{3}-\frac{2}{3}\right), \tag{A11}$$

By requiring $C^S_n=0$ at the stationary state, we can determine ρ, θ_0, and μ_0 as a function of l_0. To find ρ, θ_0, and μ_0, we need the continuum limit of

$$\prod_{k=0}^{l} b_{n+k}\doteq\rho^{l+1}-\frac{1}{2}\rho^l(l+1)D+\rho^{l-1}\frac{l+1}{8}(l+4\rho\theta_0)D^2+\rho^l\frac{l+1}{4}(2\mu_0-l)\partial D. \tag{A12}$$

We determine $\rho(l_0)$ from Eq. (20). ρ is the solution of the equation

$$2x^2-4x+1-x^{2l_0+1}[1-x(5+2l_0)+x^2(3+2l_0)]=0, \tag{A13}$$

whose approximate solution is

$$\rho(l_0)\approx\rho_\infty\left[1+\tfrac{1}{4}\rho_\infty^{2l_0+1}(2l_0+1)\right]+O(\rho_\infty^{4l_0}), \tag{A14}$$

with $\rho_\infty=(2-\sqrt{2})/2$, which is the solution for infinite l_0. By the same reasoning, we can find θ_0 and μ_0, whose approximate solutions read

$$\theta_0(l_0)\approx\frac{\sqrt{2}}{4}\left[1+\rho_\infty^{2l_0}\left(\frac{6-5\sqrt{2}}{4}+\frac{21-17\sqrt{2}}{6}l_0+\frac{2-\sqrt{2}}{2}l_0^2+\frac{\sqrt{2}}{3}l_0^3\right)\right]+O(\rho_\infty^{4l_0}),$$
$$\mu_0(l_0)\approx\frac{4-3\sqrt{2}}{4}\left[1+\rho_\infty^{2l_0}\left(-\frac{3\sqrt{2}}{4}+\frac{4-17\sqrt{2}}{12}l_0+\frac{2+\sqrt{2}}{2}l_0^2+\frac{2+2\sqrt{2}}{3}l_0^3\right)\right]+O(\rho_\infty^{4l_0}). \tag{A15}$$

For finite l_0, the most relevant terms arise from the second line of Eq. (19) and the resulting equation is the KPZ one, with coefficients

$$\nu=-\mu(2l_0+1),\quad \lambda=-2\theta(2l_0+1). \tag{A16}$$

We give the numerical values of ρ, ν, and λ in the table. These numbers are determined from the direct calculation of ρ, θ_0 and μ_0 using Eq. (19). These λ's should be compared with the previous numerical results [14]. Note that λ in Ref. [14] is one half of λ here.

For infinite l_0, the second line of Eq. (19) vanishes, of which the physical meaning is that a dropped particle even-

tually finds a stable site. Hence the continuum equation becomes the VLD equation with coefficients

$$\tilde{\nu} = -\frac{1}{2}\sum_{j=1}^{\infty} j\mu(j), \qquad \tilde{\lambda} = \frac{1}{2}\sum_{j=1}^{\infty} j\theta(j). \tag{A17}$$

APPENDIX B: DISAPPEARANCE OF ODD POWERS OF *D* IN *R*

This appendix proves that the first line of Eq. (19) does not generate terms $\partial^2(\partial h)^{2i+1}$, where i is a non-negative integer. To this end, consider a Taylor expansion of R^l_{n+k} and set the lattice constant to be 0. We call this quantity $T^{l_0}_l(D)$, and the corresponding quantity for $S\,S_{l_0}(D)$. One should not confuse this procedure with the continuum limit. It is enough to prove that $T^{l_0}_l(-D) = T^{l_0}_l(D)$. It is clear that $T^{l_0}_l(D)$ has no k dependence because the lattice constant is set to 0. This fact enables us to write the recursion relation of $T^{l_0}_l(D)$ in the symmetric form

$$\begin{aligned} 2T^{l_0}_l(D) = {} & S_{l_0}(D)T^{l_0}_{l-1}(D) + \left(1 - \frac{S_{l_0}(D)+D}{2}\right) \\ & \times \left(\frac{S_{l_0}(D)-D}{2}\right)^l + \left(1 - \frac{S_{l_0}(D)-D}{2}\right) \\ & \times \left(\frac{S_{l_0}(D)+D}{2}\right)^l . \end{aligned} \tag{B1}$$

Hence we see that

$$2[T^{l_0}_l(D) - T^{l_0}_l(-D)] = S_{l_0}(D)[T^{l_0}_{l-1}(D) - T^{l_0}_{l-1}(-D)]. \tag{B2}$$

The mirror symmetry of this system restricts the form of S_{l_0} to be even in D, so $T^{l_0}_{l-1}(D) = T^{l_0}_{l-1}(-D)$ implies $T^{l_0}_l(D) = T^{l_0}_l(-D)$. Indeed $T^{l_0}_1(D) = S_{l_0} + (S^2_{l_0} - D^2)/4$ and the logic of the mathematical induction proves the disappearance of the odd powers of D in $T^{l_0}_l(D)$. The vanishing $\gamma(l,k)$ in Appendix A is a consequence of this property. As a result, we can safely affirm that the CRSOS model is described by the VLD equation.

[1] For a review, see, e.g., A.-L. Barabási and H. E. Stanley, *Fractal Concepts in Surface Growth* (Cambridge University Press, Cambridge, 1995).

[2] F. Family and T. Vicsek, J. Phys. A **18**, L75 (1985).

[3] A. Pimpinelli and J. Villain, *Physics of Crystal Growth* (Cambridge University Press, Cambridge, 1999).

[4] M. A. Herman and H. Sitter, *Molecular Beam Epitaxy: Fundamentals and Currents Status* (Springer-Verlag, Berlin, 1989).

[5] D. D. Vvedensky, A. Zangwill, C. N. Luse, and M. R. Wilby, Phys. Rev. E **48**, 852 (1993).

[6] K. Park and B. Kahng, Phys. Rev. E **51**, 796 (1995).

[7] M. Přeodota and M. Kotrla, Phys. Rev. E **54**, 3933 (1996).

[8] Z.-F. Huang and B.-L. Gu, Phys. Rev. E **57**, 4480 (1998).

[9] S.-C. Park, D. Kim, and J.-M. Park, Phys. Rev. E **62**, 7642 (2000).

[10] S. F. Edwards and D. R. Wilkinson, Proc. R. Soc. London, Ser. A **381**, 17 (1982).

[11] M. Kardar, G. Parisi, and Y.-C. Zhang, Phys. Rev. Lett. **56**, 889 (1986).

[12] Y. Kim, D. K. Park, and J. M. Kim, J. Phys. A **27**, L533 (1994).

[13] J. Villain, J. Phys. I **1**, 19 (1991); Z.-W. Lai and S. Das Sarma, Phys. Rev. Lett. **66**, 2348 (1991).

[14] Y. Kim and S. H. Yook, J. Phys. A **30**, L449 (1997).

[15] J. Neergaard and M. den Nijs, J. Phys. A **30**, 1935 (1997).

[16] A. K. Kshirsagar and S. V. Ghaisas, Phys. Rev. E **53**, R1325 (1996).

[17] J. M. Kim and J. M. Kosterlitz, Phys. Rev. Lett. **62**, 2289 (1989).

[18] J. M. Kim and S. Das Sarma, Phys. Rev. Lett. **72**, 2903 (1994).